

Effect of Li Content on Properties and Microstructure Evolution of Near-Rapid Solidified 2A97 Al-Li Alloy

Tang Yingchun¹, Luo Lei¹, Luo Liangshun¹, Liu Yulin², Xu Yanjin³,
Su Yanqing¹, Guo Jingjie¹, Fu Hengzhi¹

¹ National Key Laboratory for Precision Hot Processing of Metals, Harbin Institute of Technology, Harbin 150001, China; ² Shenyang Aerospace University, Shenyang 110100, China; ³ AVIC Manufacturing Technology Institute, Beijing 100024, China

Abstract: 2A97 Al-Li alloys with different Li contents were cast by the near-rapid solidification. After that, physical properties analysis was performed by tensile and density tests. Simultaneously, the differential scanning calorimeter (DSC), optical microscope (OM), scanning electron microscope (SEM) and energy dispersive spectrometer (EDS) were used to explore the microstructure evolution of the Al-Li alloy. The results show that the near-rapid solidification and a reasonable heat treatment process can effectively reduce the coarse second phase in the 2A97 Al-Li alloy, which is of great significance for obtaining ultra-low-density Al-Li alloys. With the increase of Li content, the Cu element in the alloy is more inclined to capture more Li element to form the Al₂CuLi phase. Accompanied by the relative decrease of Al₂Cu phase, the petal-shaped eutectic phase Al₂CuMg appears. Besides, the as-cast microstructure of the near-rapid solidified Al-Li alloy transforms from dendritic grains to cellular-like grains, leading to the refinement of the grains. However, as the Li content increases from 1.5 wt% to 3.5 wt%, the effect of the heat treatment decreases sharply, resulting in many coarse eutectic phases remaining in the triangular cross boundaries of the alloy and a reduction in mechanical properties of alloys.

Key words: 2A97 Al-Li alloys; near-rapid solidification; ultra-low-density Al-Li alloys; petal-shaped eutectic phase

Al-Li alloy has gradually become a structural material with great application potential in aerospace because of its light weight, low anisotropy, high elastic modulus, high strength and good age hardening characteristics^[1,2]. Studies have shown that for every 1 wt% of Li added, the density of the alloy can be reduced by 3%, while the elastic modulus can be increased by 6%^[3,4]. Li element can play a significant strengthening role in the alloy because of solid solution strengthening and δ' precipitation strengthening^[5]. Appropriately increasing the solid solution limit of Li in the alloy is of great significance for improving the properties of the alloy. In the history of Al-Li alloys, there are three generations. Among them, Li content of the second-generation Al-Li alloy is 1.9%~2.7%, making the alloy density lower, the elastic modulus higher, the fatigue life longer, and the crack growth rate slower^[6]. However, due to the increase of Li element, the

anisotropy of the alloy is aggravated and the segregation of specific gravity is increased. In the aging process, the δ phase will be generated at the grain boundary. During the growth of the grain boundary phase, a small uniform δ' phase will be consumed, leading to a serious reduction in the fracture toughness^[7]. Therefore, the third-generation Al-Li alloy appropriately reduces the Li content but increases the Cu content to improve the alloy performance^[8,9]. However, this method has led to a limitation in the reduction of the density of Al-Li alloys, making it impossible to obtain ultra-low-density Al-Li alloys.

Currently, researches on improving the performance of Al-Li alloy mainly focus on age-hardening. Deng et al^[10] carried out research on the rolling process of Al-Cu-Li after aging. And the results show that Al-Cu-Li alloys processed through cryogenic rolling followed by aging treatment can get better

Received date: September 10, 2019

Foundation item: National Natural Science Foundation of China (51671073); National Key Research and Development Program of China (2016YFB0301201)

Corresponding author: Luo Liangshun, Ph. D., Associate Professor, National Key Laboratory for Precision Hot Processing of Metals, School of Materials Science and Engineering, Harbin Institute of Technology, Harbin 150001, P. R. China, Tel: 0086-451-86413910, E-mail: luolei900303@163.com

Copyright © 2019, Northwest Institute for Nonferrous Metal Research. Published by Science Press. All rights reserved.

mechanical properties, which not only have high strength but also good ductility. Deschamps et al.^[11] studied the microstructure evolution of Al-Cu-Li alloy with different Li contents during aging. The results indicate that the δ phases in the alloy with high Li content evolve into a large number of δ' phases during long-term aging. Some relevant studies have found that by suitable homogenization process, dendrite segregation and non-equilibrium eutectic phases in the alloy can be effectively eliminated^[7,12], which has significant implication for improving the properties of the alloy.

However, the current study on the performance improvement of Al-Li alloys still takes the third-generation Al-Li alloy, a low-Li-content (<1.8%) aluminum-lithium alloy, as an object. The research of increasing the Li content in the Al-Li alloy to greatly reduce the alloy density while ensuring the alloy microstructure and performance and finally obtaining ultra-low-density Al-Li alloy on the basis of the special solidification technology and effective heat treatment process, is still relatively less.

In this paper, 2A97 Al-Li alloys with different Li contents were prepared by near-rapid solidification, and the anisotropy of the alloy caused by the increase of Li content was improved by the relevant heat treatment process. The aim is to increase the addition amount of Li in Al-Li alloys by combining special solidification technique with suitable heat treatment, and to ensure the excellent microstructure and properties of the alloy, providing a new idea for the realization of ultra-low-density Al-Li alloys.

1 Experiment

The experimental material was based on Al-XLi-4.5Cu-0.5Mg-0.12Zr-0.5Zn-0.5Mn (X=1.5, 2.5, 3.5, wt%). The Li content in the alloy was adjusted appropriately. The chemical composition of the experimental alloy is shown in Table 1.

High-purity Al, high-purity Li, master alloy Al-Mg, Al-Zn, Al-Cu and Al-Zr were used as raw materials for alloy preparation. The high-purity Al was placed in an electric resistance furnace and smelted at a melting temperature of 710 °C. After Al melting was finished, Cu, Zn, Zr and Mg were added. Then, degassing was carried out using C₂Cl₆ and high purity Ar, followed by the addition of Li element. High-purity Li was wrapped in aluminum foil and was pressed to the bottom of the molten alloy using a bell-type feeding device. In this process, anhydrous lithium chloride was used as a covering agent. Then, 0.1% alloy grain refiner (Al₅TiB) of the total amount of alloy was added. After the alloy elements were completely melted, the alloy was cast after 5 min of heat preservation.

Table 1 Chemical composition of Al-Li alloys (wt%)

Alloy	Li	Mn	Cu	Mg	Zr	Zn	Al
1#	1.51	0.51	4.50	0.49	0.12	0.50	Bal.
2#	2.49	0.49	4.49	0.51	0.12	0.50	Bal.
3#	3.49	0.49	4.51	0.50	0.13	0.51	Bal.

The schematic of the near-rapid solidification device is shown in Fig.1. The pouring process used gate and riser for feeding. The outer wall of the mold was sprayed with water to reach a near-rapid solidification rate. Argon gas protection and a real-time temperature measurement by temperature collector were performed during the entire casting process. Finally, a plate-shaped ingot with a size of 200 mm×150 mm×15 mm was obtained. The ingot was cut and processed. After that, heat-treatment, mechanical properties test, density test and microstructure analysis were performed.

The density of samples was measured 3 times by the high-precision digital density meter QL-202GR and then averaged. Before the test, several small pieces of as-cast sample with the dimension of 15 mm×15 mm×4 mm were cut. And the surface of each sample was polished with 240#~1000# sandpaper to eliminate stain and obvious defects. The DSC test was performed using STA449F3 TG/DSC simultaneous thermal analyzer. Heating rate was 40 °C/min. When the temperature reached 720 °C, the samples were held for 15 min, and then cooled down at a rate of 2 °C/min. Tensile properties were measured on a CMT-5105 universal testing machine at a tensile rate of 1 mm/min. The diameter of the sample was 12 mm and the gauge length was 60 mm. The extensometer was added during the experiment. Each group of three samples was averaged. The sample was electro-polished and then placed in a polishing solution of HClO₄+H₂O+C₂H₅OH at a polishing voltage of 27 V DC for 1s, followed by observation and analysis of metallographic microstructure using OLYMPUS GX71 optical microscope (OM) and Quanta 200FEG (FEI) scanning electron microscope (SEM) equipped with EDS.

2 Results and Discussion

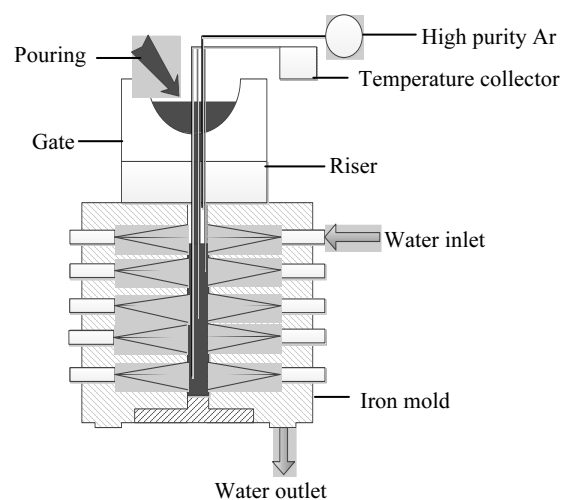


Fig.1 Near-rapid solidification device

2.1 DSC analysis

The more low-melting-point elements are added, the lower the phase transition temperature of the alloy. Therefore, the sample with 3.5 wt% Li was chosen for DSC test, while, the 1.5 wt% Li contained sample was used for heat-treatment temperature test. The DSC curve and the heat-treatment temperature test result are shown in Fig.2.

From the DSC curve shown in Fig.2a, the last exothermic peak of the alloy appears at about 520 °C, the starting point appears at about 510 °C, while the end temperature is about 530 °C. Heat preservation for 1# Al-Li alloy was performed at 530 °C for 24 h as a homogenization heat treatment. Traces of over-burning in the microstructure were found, as shown by area A in Fig.2b. According to the analysis of DSC result and related studies, the dissolved temperatures of Al_2CuMg phase and Al_2Cu phase are 495 and 515 °C, respectively^[13]. Therefore, the temperature of the heat treatment system cannot exceed 520 °C.

Aging processes can affect the δ' phase in Al-Li alloys, resulting in corresponding changes of alloy properties. In the under-aging and peak-aging processes, the δ' phase dimension is small, and a large amount of T_1 phase will precipitate in the matrix. As a result, no second phase precipitates in the grain boundary, bringing an improvement in the alloy mechanical properties. As a comparison, when over-aging, the δ' phase dimension is larger, resulting in a decrease in the alloy strength and toughness^[14]. The final determination of the experimental methods and heat-treatment processes are shown in Fig.3.

2.2 Effect of Li content on microstructure of Al-Li alloys

The different Li contents can lead to obvious differences in metallographic microstructure of alloy. As shown in Fig.4, the microstructure of the samples cast by the near-rapid solidification was compared with that of samples with the heat-treatment.

By calculating the results of the temperature acquisition instrument, the cooling rate in this experiment can reach 200 K/s. The related studies of Al-Li alloys show that when the Li content is less than 0.5 wt%, only the θ' phase precipitates in the alloy. When the Li content reaches 0.5 wt%~1.1 wt%, the θ' phase and the T_1 phase are precipitated. When the Li content is more than 2.1 wt%, the θ' phase, the T_1 phase and the δ' phase are all precipitated. When the cooling rate is high, a non-equilibrium solidification reaction occurs. In this condition, when the Li element is 1.5 wt%, the production of the δ' phase may occur. By comparing the as-cast microstructures of the specimens in Fig.4a, 4c and 4e, it can be concluded that dendritic segregation occurs in the metallurgical microstructure of the alloy when the Li content is 1.5 wt%. The second phases mainly concentrate at the triangular cross boundaries and form the low-melting eutectic phase. This is because near-rapid solidification has a high cooling rate and a high degree

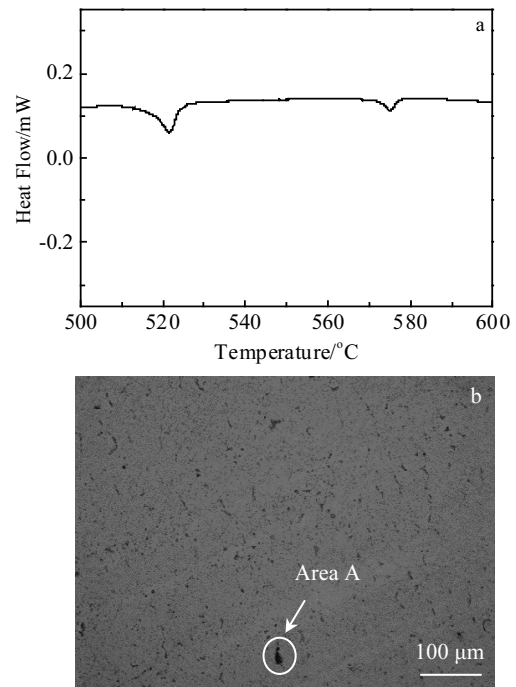


Fig.2 DSC curve of sample with 3.5 wt% Li (a) and microstructure (b) of 1.5 wt% Li contained sample after insulating at 530 °C for 24 h

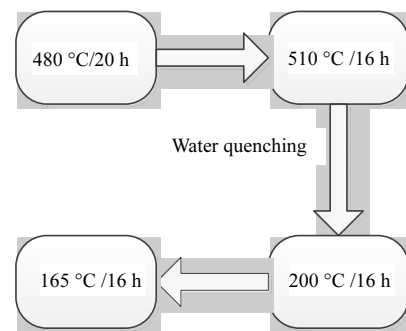


Fig.3 Heat-treatment process

of undercooling, so that the alloy is easily subjected to non-equilibrium eutectic reactions^[15]. Subsequently, the solute atoms begin to segregate and undergo a eutectic reaction: $\text{L} \rightarrow \alpha(\text{Al}) + \text{T}_2(\text{Al}_6\text{CuLi}_3)$. The T_2 phase is small and more easily dispersed. When the content of Li reaches 2.5 wt%, the alloy begins to exhibit a metallographic structure in which dendrites and cellular-like grains coexist. As the Li content increases to 3.5 wt%, almost all the grain microstructures of the alloy are cellular-like grains, so-called equiaxial grains. In general, with the increase of the Li content, the microstructure changes from the dendrite to the cellular-like grain, and the

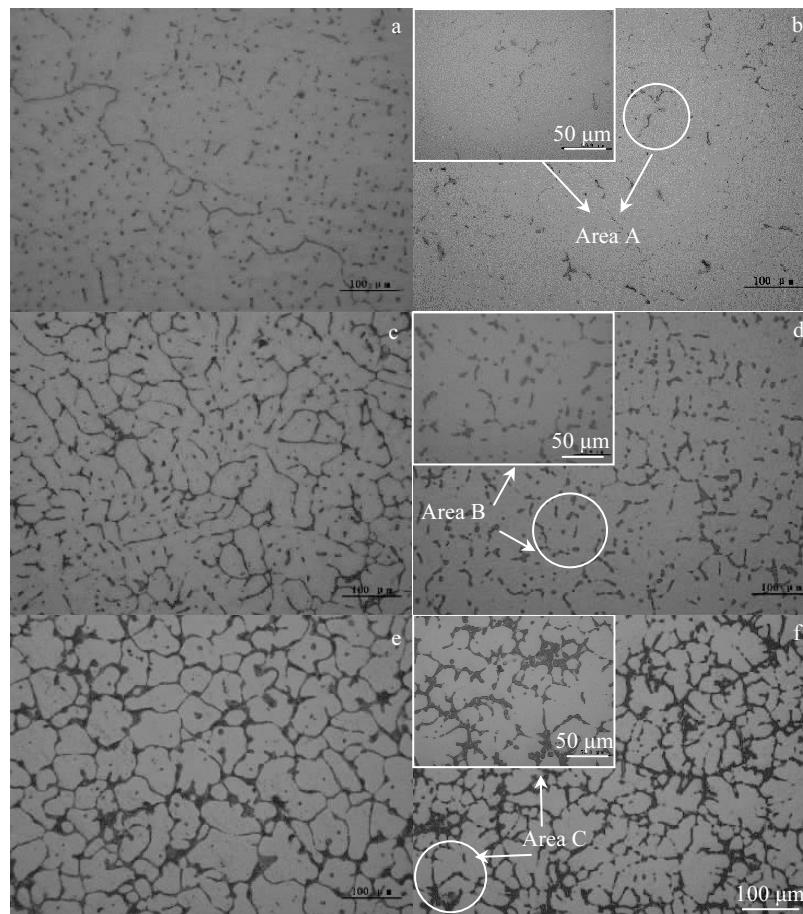


Fig.4 Metallographs of as-cast (a, c, e) and heat-treated (b, d, f) samples with different Li contents: (a, b) 1#, (c, d) 2#, and (e, f) 3#

larger grains are disassembled into many smaller particles. In the triangular cross boundaries, more unmelted second phases appear gradually and are distributed unevenly.

Fig.4 compares the as-cast microstructures micrographs after heat-treatment; it shows that the dendritic grains and cellular-like grains in the as-cast microstructure are almost completely re-dissolved by heat treatment at a Li content of 1.5 wt% and 2.5 wt%. The broken grains are diffusely distributed in the matrix, leaving only a small amount of grains in the triangular cross boundaries of the microstructure, which results in homogenization of the alloy as well as improvement of the mechanical performance. While, when the Li content reaches 3.5 wt%, there are a mass of coarse second phases left.

By comparing the photomicrographs of the three groups of specimens after heat treatment in Fig.4b, 4d and 4f, it can be found that for the same heat treatment system, alloys with lower Li content are more effective. Through the heat treatment process, a large number of the coarse phases at the grain boundaries are re-dissolved, leaving the fine uniform precipitate phases mainly including the δ' phase, the θ' phase, the S' phase, and the T_1 phase^[14]. With the increase of Li content,

the effect of heat treatment begins to decrease. At this time, the coarse phase in the grain boundary position cannot be completely eliminated, and more coarse phases remain. Moreover, aggregated lamellar coarse phases gradually form at the interdigitated triangle positions.

The SEM images and EDS analysis are shown in Fig.5 and Table 2, respectively.

By analyzing the SEM photographs and EDS analysis in Fig.5a, 5b and Table 2, it is indicated that when the Li content is 1.5 wt%, after heat-treatment, the main components of the residual phases are Al, Mn, Fe, Cu and Zn. Among them, Fe is an impurity, and during the smelting process, it is mixed into the alloy through the iron tools such as feed clamps to form a hardly soluble impurity AlCuFeMn phase^[16]. The main structures of the non-equilibrium phases are Al_2CuLi and Al_2Cu phases containing a small amount of Mg element, like a white block. In addition, there are some η phases composed of Zn and Mg elements, which are relatively coarse and mainly distributed at grain boundaries.

By analyzing the SEM photographs and EDS analysis in Fig.5c, 5d and Table 2, it can be found that when the Li content is 2.5 wt%, after heat-treatment, the main components of

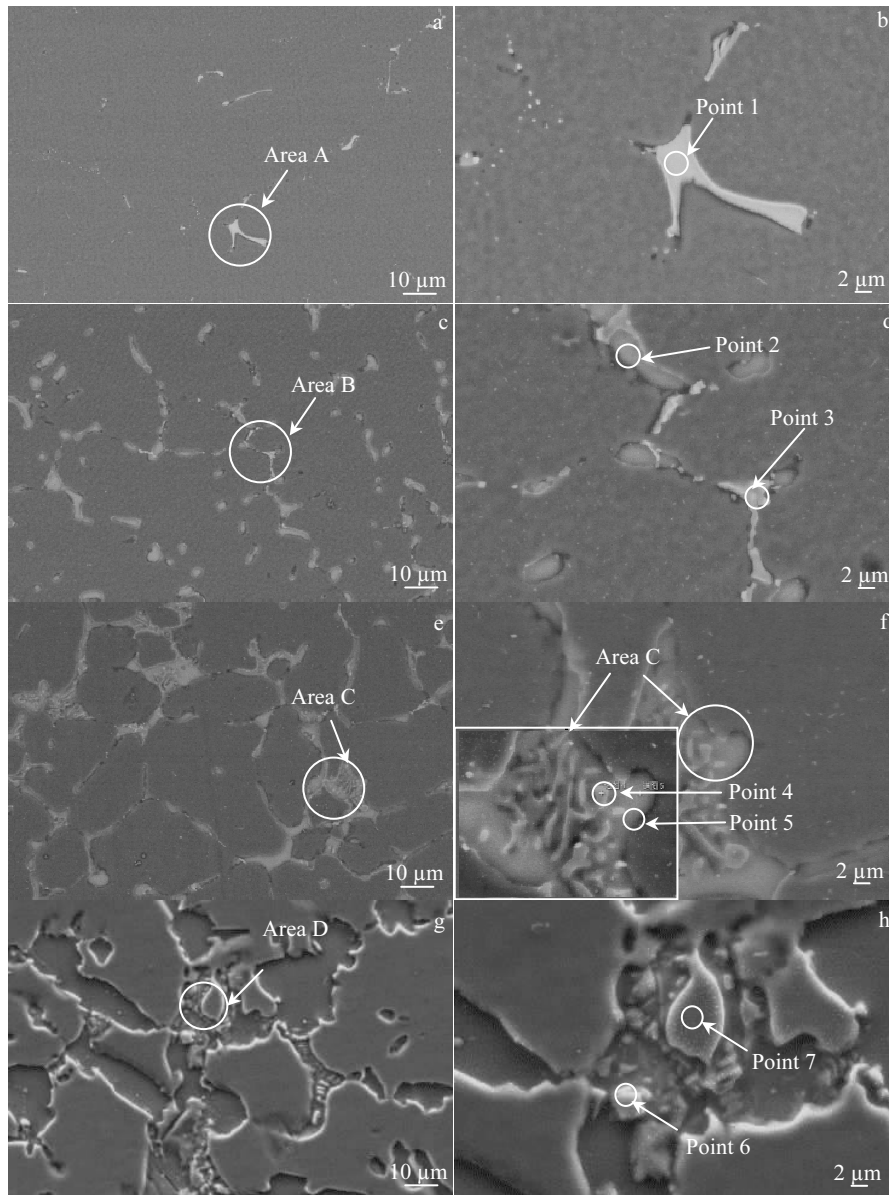


Fig.5 SEM images of samples containing 1.5 wt% (a, b), 22.5 wt% (c, d) and 3.5 wt% (e~h) Li: (a) after heat-treatment and (b) magnification of area A; (c) after heat-treatment and (d) magnification of area B; (e) after heat-treatment and (f) magnification of area C; (g) as-cast and (h) magnification of area D

Table 2 EDS analysis of points in Fig.5 (wt%)

Point	Mn	Cu	Mg	Zr	Zn	Al	Fe
1	6.77	36.60	-	-	1.67	46.40	8.56
2	0.14	33.00	1.89	0.09	2.63	60.24	2.00
3	9.67	18.13	0.03	-	0.48	59.11	12.57
4	0.08	21.79	0.46	-	2.38	66.63	8.66
5	0.20	25.98	0.80	0.14	3.25	60.07	9.55
6	0.12	23.38	0.50	-	2.41	68.42	5.17
7	0.17	24.88	0.67	0.11	2.98	62.72	8.47

the residual phase are Al, Mg, Mn, Fe, Cu, Zn. The impurity phase is AlCuFeMn phase. Point 2 shows that the precipitated phases contain Mg element. The main compositional phases are Al_2CuMg phase and Al_2CuLi phase, in a gray block shape. Point 3 shows that the phases are Al_2Cu , Al_2CuLi , a small amount of $\text{Al}_{20}\text{Cu}_2\text{Mn}_3$, and a partially coarse η phase. Otherwise, the precipitated phases mainly exhibit a white block shape.

From Fig.5e, 5f and Table 2, it is indicated that when the Li content reaches 3.5 wt%, the petal-shaped eutectic phase ap-

appears at the triangular cross boundaries of the microstructure. By spectrum analysis, it can be determined that the phase mainly includes Al_2CuLi phase, Al_2Cu phase and Al_2CuMg phase combined with some eutectic phases and some coarse η phases. As a comparison, the fact that the Al_2CuLi phase, Al_2Cu phase and Al_2CuMg phase appears in the microstructure at the very beginning and cannot be completely eliminated by the heat-treatment can be concluded from Fig.5g, 5h and Table 2. These undissolved precipitation phases are unevenly distributed and converge at the triangular cross boundaries. The morphology of the precipitated phases also shows irregular block shape and petal shape, resulting in poor bonding of the alloy phase interface. As a result, these areas become the best areas for crack propagation, so the alloy performance is deteriorated.

By comparing Fig.5a, 5c and 5e, it can be seen that when the Li content is 1.5 wt%, the Cu content is relatively high, and the second phases are mainly composed of Al_2CuLi phase and a small amount of Al_2Cu phase in which the Mg element is dissolved. As the Li content increases, the Cu element in the alloy combines with more Li element, resulting in an increase in the Al_2CuLi phase and a relative decrease in the Al_2Cu phase. This promotes the formation of Al_2CuMg phase and more petal-shaped eutectic phases. Under the same heat-treatment processes, when the Li content reaches 3.5 wt%, more coarse eutectic phases are remained at the triangular cross boundaries in the microstructure of the alloy, leading to a decrease in the alloy performance. The heat-treatment process results in preferential growth of the θ' phase in the dispersed phase.

The addition of Mg element can inhibit the formation of the T_2 phase to a certain extent but promote the precipitation of the δ' phase^[7]. At the same time, Mg and Zn form coarse η

phases, which mostly appear at the grain boundary. With regards to the alloy with different Li contents, the effects achieved by the same heat treatment process are also different. As the Li element content increases from 1.5 wt% to 3.5 wt%, the composition of the as-cast microstructure of the alloy changes. Moreover, the effect of the heat-treatment decreases, and the precipitated phases of the alloy after heat treatment also change accordingly.

2.3 Effect of Li content on density and mechanical properties of Al-Li alloys

The fracture scanning images of the specimens are shown in Fig.6. At the same time, the density test results and tensile properties of the three sets of specimens are shown in Table 3.

By comparing the fracture scanning images of the three groups of specimens in Fig.6, it can be seen that all the specimens exhibit typical brittle fracture features. And when the Li content reaches 3.5 wt%, many inclusion phases appear in the fracture microstructure. These phases cannot be re-dissolved by the same heat treatment, and become the origin of propagation for cracks, resulting in non-uniform properties and poor mechanical properties.

As shown in Table 3, the increase of Li content has an obvious alloy density reduction effect. It indicates that the Li element has very great potential for alloy density reduction effect the realization of the ultra-low-density Al-Li alloys. However, as the Li content increases, the tensile strength and the elongation of the Al-Li alloy drop sharply under the same heat treatment, while, the alloys become very brittle.

Combining the analysis of Fig.4~6, it can be concluded that as the Li element increases, the alloy phase component is deflected. When the Li content is as low as 1.5 wt%, the major phases in the alloy are the δ' phase, the θ' phase, the

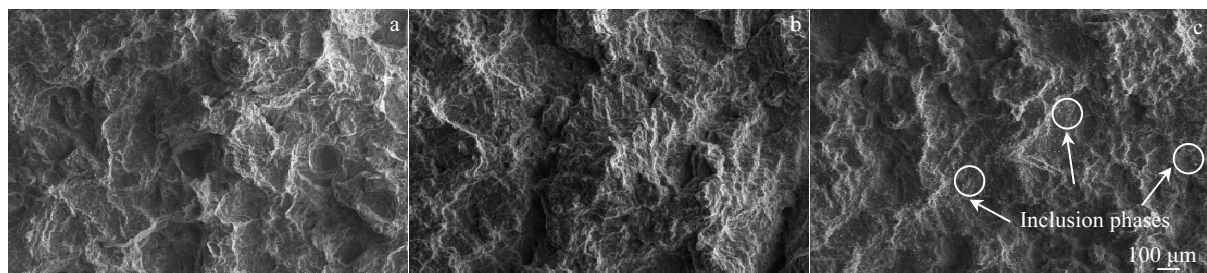


Fig.6 SEM images of the fractures of specimens containing different Li contents after heat-treatment: (a) 1#, (b) 2#, and (c) 3#

Table 3 Density and tensile properties of Al-Li alloys

Specimen	σ_b/MPa	$\delta/\%$	$\rho/\text{g}\cdot\text{cm}^{-3}$
1#	430.01	4	2.66
2#	400.12	4	2.61
3#	212.10	3	2.53

S' phase, and the T_1 phase^[17]. Because of the high binding energy between the nuclear vacancies and Li atoms, the aggregation of vacancies is inhibited, making it impossible to form dislocation loops. The possible non-uniform nucleation sites are only grain boundaries and sub-grain boundaries. While, Mg element inhibits the formation of θ' phase and precipitates the S' phase. This phase promotes more uniform distribution of dislocation slips, which is beneficial to the fatigue proper-

ties of the alloy. When the Li element is too high, it will cause the microstructure to change from the T_1 phase to the T_2 phase, which will mostly precipitate at the high-angle grain boundaries. As a result, a non-precipitation zone of the δ' phase near the grain boundaries appears. Eventually, fracture toughness of the alloy is decreased^[18]. According to Table 3, it can be seen that when the Li content is 2.5 wt%, although the tensile strength of the 2# model is lower than that of the 1# model due to the lower effect of the same heat-treatment, the effect of the density reduction is more significant. According to Fig.6b, there are not many inclusion precipitation phases. From Fig.5, it still can be concluded that when the Li content is 2.5 wt%, under the same heat treatment process, there is no large petal-shaped eutectic phase, indicating that better uniformity can be achieved by the special cast technique and appropriate heat-treatment.

3 Conclusions

1) Near-rapid solidification technology and reasonable heat-treatment process can effectively eliminate the coarse second phase in the 2A97 Al-Li alloys, which helps to increase the amount of Li addition in the alloy and reduce the alloy density.

2) With the increase of Li content, the as-cast microstructure of the near-rapid solidified Al-Li alloys transforms from dendritic grains to cellular-like grains. Simultaneously, large grains are obviously refined.

3) Under the same heat-treatment process, the Al-Li alloys with a lower Li content of 1.5 wt% have more obvious heat-treatment effect and higher mechanical properties. With the increase of Li content, the effect of the heat treatment gradually decreases. When the Li content is as high as 3.5 wt%, the heat-treatment at this time is almost ineffective, resulting in a serious decline in mechanical properties. At the same time, the higher the Li content, the lower the Cu/Li ratio, resulting in an increase of the Al_3Li phase and a relative decrease of the Al_2CuLi phase, which also leads to a loss in the alloy strength.

4) After the heat-treatment of the alloy, the main components of the precipitated phases include Al, Cu, Mg, Zn, Mn, and Fe. When the Li content is lower than 1.5 wt%, the precipitated phase is mainly white bulk Al_2Cu and a small amount of $Al_{20}Cu_2Mn_3$. When the Li content reaches 2.5 wt%, Al_2CuMg , Al_2Cu , and Al_2CuLi appear in the precipitated phases. This is because the increased Li forms Al_2CuLi with Cu, resulting in a decrease in the Cu content compared to the Mg content, so the formation of Al_2CuMg can be promoted. Therefore, this phenomenon that a gray phase precipitates in

the white bulk phase occurs. When the Li content reaches 3.5 wt%, the precipitated phases are almost disassembled into white and gray parts, whose shapes are similar to the petals. Al_2CuMg and Al_2CuLi are predominant in the precipitation phase at this time. These precipitated phases are irregular in shape and non-uniformly distributed, resulting in poor bonding of the alloy phase interface. As a result, these areas become the best areas for crack propagation, so the alloy performance is deteriorated.

References

- 1 Dorin T, Deschamps A, Geuser F D et al. *Acta Materialia*[J], 2014, 75: 134
- 2 Shi C L, Xi X K. *Intermetallics*[J], 2014, 51: 64
- 3 Li Jinfeng, Zheng Ziqiao, Ren Wenda et al. *Transactions of Nonferrous Metals Society of China*[J], 2006, 16(6): 1268
- 4 Li Hongying, Tang Yi, Zeng Zaide et al. *Transactions of Nonferrous Metals Society of China*[J], 2008, 18(4): 778
- 5 Gao C, Luan Y, Yu J C et al. *Transactions of Nonferrous Metals Society of China*[J], 2014, 24(7): 2196
- 6 Rioja R J, Liu J. *Metallurgical & Materials Transactions A*[J], 2012, 43(9): 3325
- 7 Zhao Zhongkui. *Microstructure and Properties of Lithium Containing Aluminum Alloys*[M]. Beijing: National Defense Industry Press, 2013
- 8 Decreus B, Deschamps A, Geuser F D et al. *Acta Materialia*[J], 2013, 61(6): 2207
- 9 Malard B, Geuser F D, Deschamps A. *Acta Materialia*[J], 2015, 101: 90
- 10 Deng Y J, Huang G J, Cao L F et al. *Transactions of Nonferrous Metals Society of China*[J], 2017, 27(9): 1920
- 11 Deschamps A, Garcia M, Chevy J et al. *Acta Materialia*[J], 2017, 122: 32
- 12 He Lizhi, Li Xiehua, Zhang Haitao et al. *Rare Metal Materials and Engineering*[J], 2010, 39(1): 107 (in Chinese)
- 13 Yang S, Jian S, Yan X et al. *Rare Metal Materials and Engineering*[J], 2017, 46(1): 28
- 14 Lin Y, Zheng Z Q, Zhang H F et al. *Transactions of Nonferrous Metals Society of China*[J], 2013, 23(6): 1728
- 15 Cui Zhongqi, Liu Beixing. *Metallurgy and Heat Treatment Theory*[M]. Harbin: Harbin Institute of Technology Press, 2004
- 16 Zhang Long, Zheng Ziqiao, Li Jingfeng et al. *Rare Metal Materials and Engineering*[J], 2016, 45(11): 3015 (in Chinese)
- 17 Zhang Saifei, Zeng Weidong, Yang Wenhua et al. *Rare Metal Materials and Engineering*[J], 2015, 44(8): 2024 (in Chinese)
- 18 Fan Chunping, Zheng Ziqiao, Jia Min et al. *Rare Metal Materials and Engineering*[J], 2015, 44(1): 91 (in Chinese)

Li 含量对亚快速凝固 2A97 铝锂合金的性能及组织演变规律的影响

唐迎春¹, 罗 磊¹, 骆良顺¹, 刘玉林², 徐严谨³, 苏彦庆¹, 郭景杰¹, 傅恒志¹

(1. 哈尔滨工业大学 金属精密热加工国家级重点实验室, 黑龙江 哈尔滨 150001)

(2. 沈阳航空航天大学, 辽宁 沈阳 110100)

(3. 中航工业制造技术研究院, 北京 100024)

摘 要: 通过亚快速凝固技术铸造 2A97Al-Li 合金, 借助密度和拉伸测试对合金性能进行分析。同时, 利用差热分析 (DSC), 光学显微镜 (OM), 扫描电镜 (SEM) 及能谱 (EDS) 对合金显微组织演变进行研究。结果表明: 通过亚快速凝固技术和合理的热处理工艺可以有效减少 2A97 Al-Li 合金中存在的粗大第二相, 这对于超低密度 Al-Li 合金的实现具有十分重要的意义。随着合金中 Li 含量的增加, Cu 原子更倾向于捕获 Li 原子而形成 Al₂CuLi 相; 同时, Al₂Cu 相相对减少, 并出现花瓣状共晶相 Al₂CuMg; 另外, 亚快速凝固 Al-Li 合金的铸态显微组织由树枝晶向胞状晶转变, 并促进晶粒细化。然而, 随着 Li 含量由 1.5% (质量分数, 下同) 上升到 3.5% 过程中, 热处理的效果逐渐降低, 导致粗大共晶相残留于合金的三角叉晶界处, 使合金力学性能降低。

关键词: 2A97 Al-Li 合金; 亚快速凝固; 超低密度铝锂合金; 花瓣状共晶相

作者简介: 唐迎春, 女, 1992 年生, 硕士, 哈尔滨工业大学材料科学与工程学院, 黑龙江 哈尔滨 150001, 电话: 0451-86413910, E-mail: tangyingchunhit@163.com